International Journal of Microwave and Wireless Technologies, 2015, 7(5), 571–577.
doi:10.1017/S1759078714000865

RESEARCH PAPER

Design of asymmetrically slotted hexagonal patch antenna for high-gain UWB applications

RAGHUPATRUNI VENKAT SIVA RAM KRISHNA[1], RAJ KUMAR[2] AND NAGENDRA KUSHWAHA[1]

A compact slot antenna for high-gain ultra wideband applications is presented. The slot is asymmetrically cut in the ground plane and is a combination of two rectangles. A hexagonal patch with two stepped coplanar waveguide-feed is used to excite the slot. The capacitive reactance of the hexagonal patch is neutralized by the inductive reactance created by the asymmetric slot and results into wider impedance matching. The measured impedance bandwidth of the proposed antenna is 11.85 GHz (2.9–14.75 GHz). The radiation patterns of the proposed antenna are found to be omni-directional in the H-plane and bi-directional in the E-plane. To enhance the gain of the antenna, a compact three-layer frequency selective surface (FSS) is used as a reflector. The overall thickness of the FSS is 3.5 mm. There is 4–5 dBi improvement in antenna gain after application of the FSS. The measured and simulated results are in good agreement.

Keywords: Antenna design, Modeling and measurements, Antennas and propagation for wireless systems

Received 24 January 2014; Revised 20 May 2014; Accepted 27 May 2014; first published online 23 June 2014

I. INTRODUCTION

Nowadays, high data transfer through wireless communication is very much in demand. This enables requirement of systems which have very wide band of frequency of operation with good quality. These types of systems require a compact high-gain antenna which offers ultra wideband (UWB) performance with cost-effectiveness and easy integration with other radio frequency (RF) circuits. Many UWB antennas have been reported in past such as UWB microstrip antenna [1–3], UWB fractal antenna [4], and coplanar waveguide (CPW)-fed UWB monopole and slot antennas [5–9]. CPW-fed slot antennas which offer UWB characteristic are more suitable for the modern wireless communication applications due to their compact size and they have an advantage that they can be easily integrated with other RF circuits. Furthermore, these antennas also offer omni-directional radiation patterns. The main disadvantage of printed UWB antennas is low gain. This problem can be addressed by incorporating a frequency selective surface (FSS) with the antenna. FSS is a periodic structure which is used to alter the propagation of electromagnetic waves. FSS can be used to enhance the gain and bandwidth of an antenna [10, 11]. The response of the FSS is determined by the shape and size of FSS. Many shapes have been designed in the past such as solid patch type, loop type, center connected, and combinations of the earlier. All the earlier shapes have disadvantage of low bandwidth. The bandwidth of an FSS can be enhanced using multiple layers of FSSs. The advantage of multilayer FSS structures is wider bandwidth and higher order transmission response. It is achieved by cascading multiple layers of FSS arrays with quarter wavelength spacing between each layer. UWB FSS have been designed with two layers [12]. But the earlier designed UWB FSSs have large size (especially in terms of thickness which is around $\lambda/4$).

In this paper, a CPW-fed slot antennas with hexagonal patch as the radiating element for UWB application is designed and proposed. The proposed antenna is compact in size and easy to design. To enhance the gain of the proposed antenna a compact FSS with three-layer metallic loop has been designed. The FSS consists of two substrate layers sandwiched between three metallic layers, and the overall thickness is very less as compare with the conventional multilayer FSSs. There is about 4–5 dBi improvement in the peak gain, about 10–15 dB reduction in back lobes and some improvement in the return loss after application of the FSS.

II. ANTENNA DESIGN

Figure 1 shows the proposed CPW-fed slot antenna. The antenna is designed on FR-4 substrate of dielectric constant 4.4 and thickness 1.6 mm. The antenna is printed on one side of the substrate. Initially, a rectangular slot is printed having dimension $W_4 \times (L_3 + L_4 + L_5)$. A double-stepped feed line having width W_{f1} and W_{f2} and a feed gap of g is used to capacitively excite the rectangular slot. The feed line

[1]Department of Electronics, DIAT (Deemed University), Pune 411025, India
[2]DIAT-ARDE, Pune, India
Corresponding author:
R. Kumar
Email: aarzoo_raj@rediffmail.com

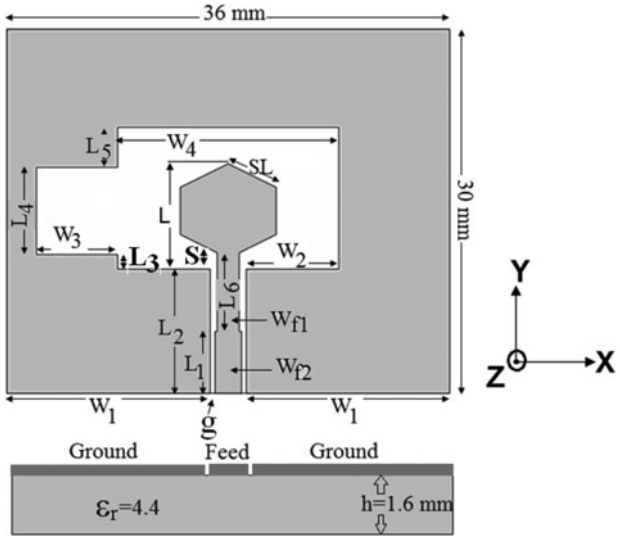

Fig. 1. Structure of the proposed antenna.

is terminated on a hexagonal patch of side length (SL). Here, double-stepped feed line is used for better impedance matching. To get efficient excitation and proper impedance matching, the combination of feed line and hexagonal patch should be well inside the rectangular slot. The length of the combination inside the slot is denoted as *L*. It has been observed that the length *L* has a significant effect on the impedance bandwidth of the capacitively coupled slot antenna. Finally, to increase the impedance bandwidth, an additional rectangular slot is incorporated in the ground plane thereby making the whole slot asymmetric with respect to the feed. The optimized dimensions of the proposed antenna are given in Table 1.

III. EXPERIMENTAL AND SIMULATED RESULTS AND DISCUSSIONS

The antenna is designed and simulated using Computer Simulation Technology (CST) Microwave Studio and then fabricated with the optimized dimensions. The reflection coefficient of the proposed antenna is measured using vector network analyzer (R&S ZVA-40). Figure 2 shows the fabricated prototype of the proposed antenna, whereas Fig. 3 shows the measured and simulated reflection coefficients. The measured impedance bandwidth of the antenna is 11.85 GHz (2.9–14.75 GHz). From the figure, it can be seen that the measured and simulated results are in good agreement. Figure 4 compares the reflection coefficient of the proposed antenna with that of an antenna without the extended slot. It can be seen from the figure that, the extended slot in the ground plane shifts the lower resonance frequency significantly toward the lower side due to an increase in overall slot length. Also, impedance matching improves due to generation of extra inductive reactance which neutralizes the capacitive reactance. So, by introducing asymmetric slot in the ground plane, compactness is achieved.

A) Theoretical discussion

Figure 5 shows the surface current distribution at different resonance frequencies. The red color shows the maximum current density, whereas blue shows minimum current density. The current distribution at 3.3 GHz shows two maxima along the slot. Then, the slot length can be approximated to one wavelength. Therefore, it can be said that the resonance at 3.3 GHz is due to the slot in the ground plane. The current distribution at 5.5 GHz shows increased current in the hexagonal patch; therefore, it can be concluded that the resonance at 5.5 GHz is due to the hexagonal patch. The current distribution at 6.5 GHz shows four maxima along the slot; therefore, it can be concluded that the resonance at 6.5 GHz is due to second harmonic of lowest resonance frequency of 3.3 GHz.

For the CPW-fed antenna considering the current distribution, the lowest frequency can be given by the following relation:

$$f_1 = \frac{300}{S_l\sqrt{\varepsilon_{eff}}}\ \text{GHz}. \tag{1}$$

Here, f_1 is the lowest resonance frequency in GHz, S_l is the effective slot perimeter in millimeter, and ε_{eff} is the effective relative permittivity. From the antenna geometry (Fig. 1), the effective slot perimeter is approximately taken as

$$S_l \approx 2\left(L_3 + L_4 + L_5\right) + 2W_4. \tag{2}$$

The second resonance frequency f_2 can be obtained by equating the effective height of the hexagonal patch to $\lambda/4$ and it is given by

$$f_2 = \frac{75}{L\sqrt{\varepsilon_{eff}}}\ \text{GHz}. \tag{3}$$

Here, f_2 is the second resonance frequency in GHz and L is the height of the hexagonal patch in millimeter. In the above expressions, ε_{eff} is the effective relative permittivity and taken to be the average of the relative permittivity of the substrate ($\varepsilon_r = 4.4$) and relative permittivity of air ($\varepsilon_r = 1$).

$$\varepsilon_{eff} = \frac{\varepsilon_r + 1}{2}. \tag{4}$$

Table 2 shows a comparison between the calculated resonance frequencies (f_1 and f_2) and simulated resonance frequencies. The calculated and simulated resonance frequencies are

Table 1. Dimensions of the proposed antenna in mm.

Parameter	W_1	W_2	W_3	W_4	L_1	L_2	L_3	L_4
Value	16.53	7.53	6.60	18.00	5.10	10.20	1.20	7.20
Parameter	L_5	L_6	g	W_{f1}	W_{f2}	SL	S	L
Value	3.30	6.90	0.39	1.80	2.16	4.36	0.90	8.70

https://doi.org/10.1017/S1759078714000865 Published online by Cambridge University Press

Fig. 2. Photograph of the fabricated antenna.

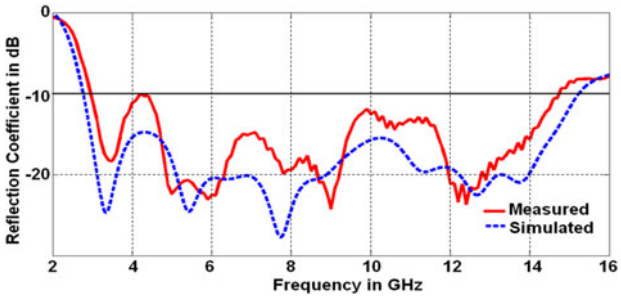

Fig. 3. Measured and simulated reflection coefficients of the proposed antenna.

differing by a value and this is because both S_L and ε_{eff} are approximate values. The exact value of ε_{eff} depends on the proportion of field distribution in substrate and air.

The open-circuit discontinuity behavior of CPW is very similar to microstrip line. In both the cases, the open circuit is capacitive [13]. The open hexagonal patch is responsible for the extra capacitance in case of proposed antenna. For the proper impedance matching, this capacitive effect needs to be neutralized. To this end, asymmetric slot is cut in the ground plane. Because of this, there is greater concentration of current in the ground near asymmetric slot and the inductance so generated compensates for patch capacitance. This

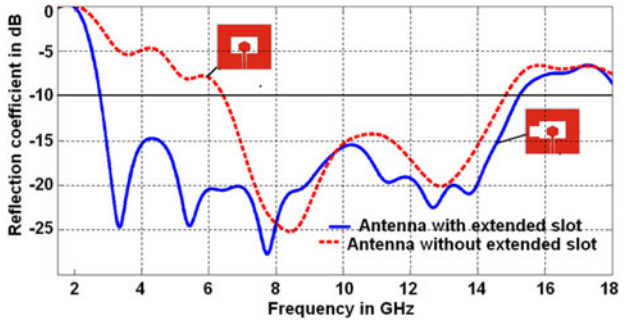

Fig. 4. Comparison of the simulated reflection coefficient of the proposed antenna with and without slots.

results in a wider impedance matching. Figure 6 shows the comparison of the real and imaginary parts of the input port impedance with and the without asymmetric slot. In the presence of an asymmetric slot, the real part of impedance shifts toward 50 Ω from higher values (in case of without asymmetric slot) and imaginary part of impedance shifts toward o value from either higher or lower values (in case of without asymmetric slot). Therefore, it can be said that the introduction of an asymmetric slot in the ground plane improves the impedance matching. Hence, a wider band antenna can be designed.

B) Radiation patterns

The radiation patterns of the proposed UWB antenna are measured in *E*-and *H*-planes in the in-house anechoic chamber using antenna measurement system. A standard double-ridged horn antenna is used as a reference antenna. The simulated and measured radiation patterns are shown in Fig. 7 for different resonance frequencies. The simulated and measured results are in good agreement. The radiation patterns in the *H*-plane are omni-directional and in the *E*-plane are bi-directional. It can be seen from the figure that the radiation patterns are also stable at higher frequencies. The radiation patterns do not deviate from bi-directionality in the *E*-plane and omni-directionality in the *H*-plane as it happens in case of other UWB antennas such as fractal antennas. By considering Fig. 7, it can be concluded that the asymmetric slot has an effect on the radiation patterns which is particularly significant at middle frequencies. The effect is only evident in the (*x*–*z*) *H*-plane. This is due to the fact that the slot is asymmetric in the *x*-direction. The *H*-plane radiation patterns at middle frequencies (Fig. 7, 5.5 and 6.5 GHz) are compressed in one direction.

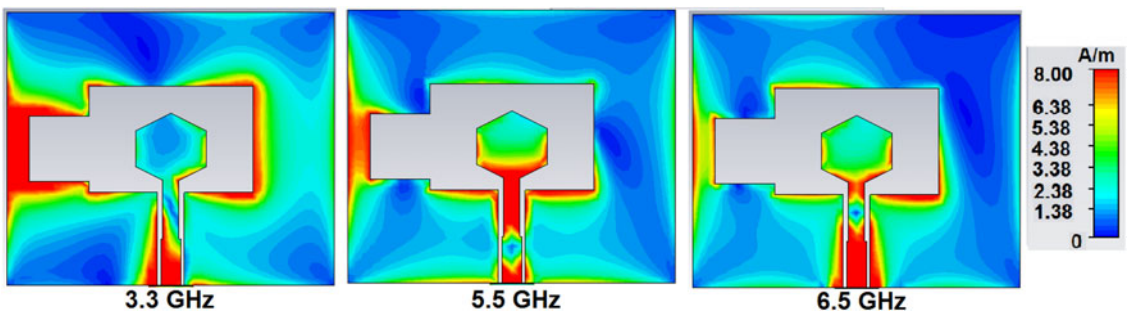

Fig. 5. Surface current distribution of the proposed antenna at different resonance frequencies.

https://doi.org/10.1017/S1759078714000865 Published online by Cambridge University Press

Table 2. Comparison of calculated and simulated resonance frequencies of the proposed antenna.

Slot size	Calculated f_1	Simulated f_1	Calculated f_2	Simulated f_2
59.40 mm	3.08 GHz	3.30 GHz	5.82 GHz	5.50 GHz

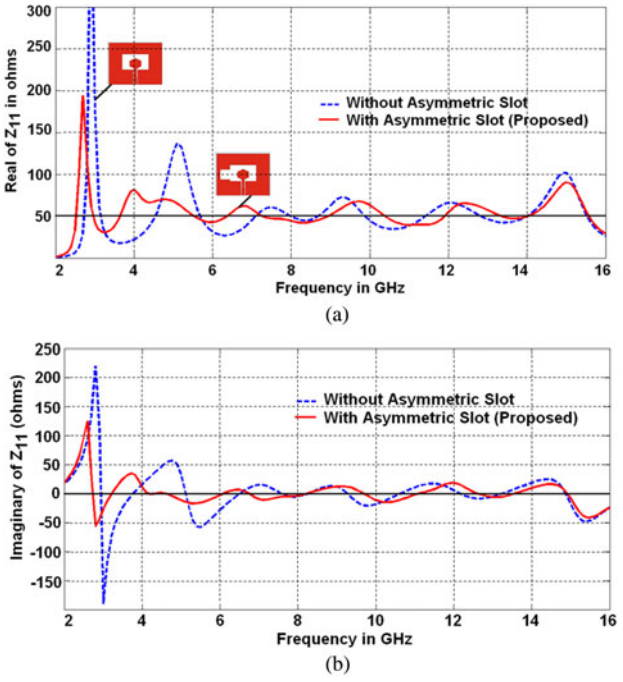

Fig. 6. (a) Comparison of the real part of the input impedance ($Z11$) of antenna without asymmetric slot and with asymmetric slot (proposed). (b) Comparison of the imaginary part of the input impedance ($Z11$) of antenna without asymmetric slot and with asymmetric slot (proposed).

IV. DESIGN OF FSS

To increase the gain of the antenna, an FSS is designed. The choice of FSS over a simple perfect electric conductor (PEC) reflector is made because though a simple PEC reflector increases the antenna gain, the variations in the gain throughout the band are found to be large. Furthermore, the impedance matching is disturbed which deteriorates the return loss characteristics over some frequencies. In comparison, an FSS has greater design freedom which helps in achieving broadband gain enhancement with little variations along with good impedance matching.

The proposed FSS is a three metallic layer structure and designed with two substrates of thickness 1.6 mm and permittivity 4.4. The unit elements are loop-type structures. The size of the unit element is same for first two layers and different for third layer. Figure 8 shows the structure of the unit elements. The dimension of the loop of the first layer (d_1) is taken to be approximately equal to half of the wavelength at the desired center frequency (6.8 GHz for frequency band from 3 to 10.6 GHz). This can be seen from the transmission characteristic with single layer (dotted green curve, Fig. 9(a)). The stop-band response of this single side FSS has a low bandwidth. Further to increase the bandwidth of the FSS, the metallic loops of same shape and size are printed on other side of the substrate. By printing on both sides, there is a significant increase in the bandwidth. But the bandwidth of the two-sided FSS is not sufficient (especially lower frequencies) to cover the entire UWB region (3.1–10.6 GHz). To cover the entire UWB region, a metallic loop with larger size (than previously used) is printed on one side of another substrate and cascaded to the earlier designed two-sided FSS. The optimized dimensions for both the loops are given in Table 3. (P_1, g_1 are periodicity and separation between unit elements for first two layers and P_2, g_2 are periodicity and separation between unit elements for the third layer).

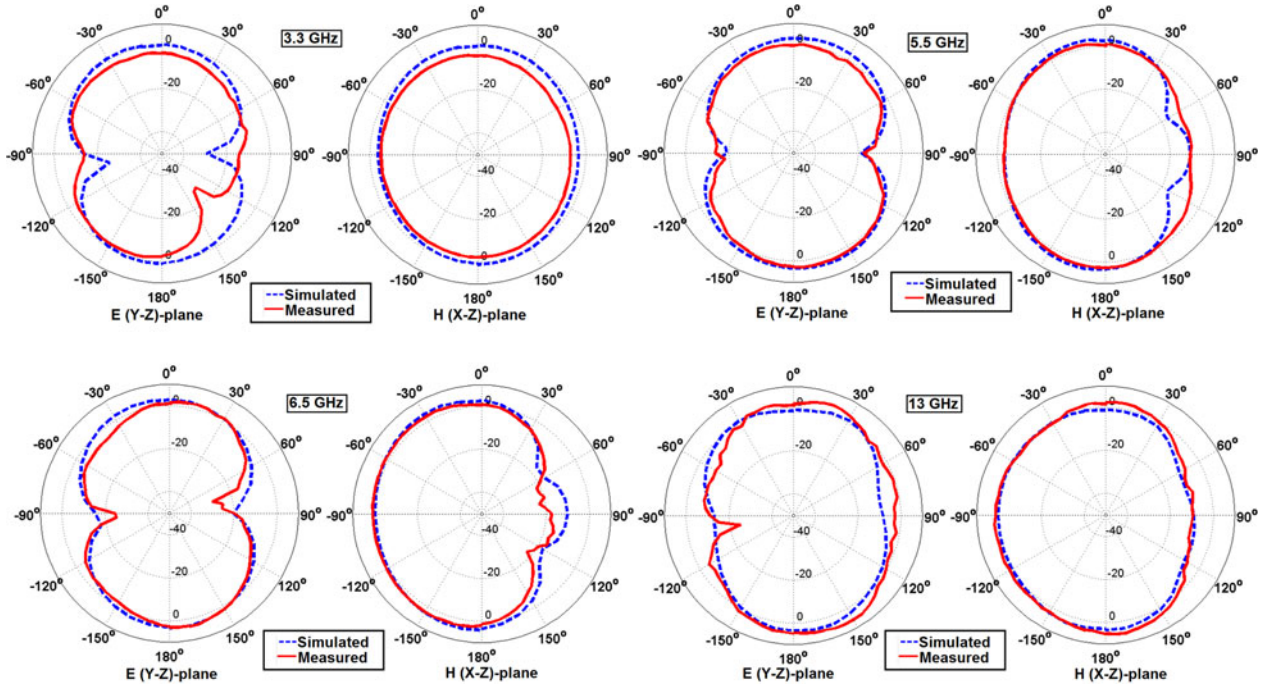

Fig. 7. Measured and simulated radiation patterns of the proposed antenna at different resonance frequencies.

https://doi.org/10.1017/S1759078714000865 Published online by Cambridge University Press

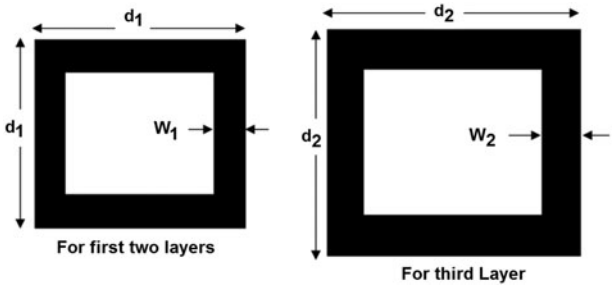

Fig. 8. Unit elements of the proposed FSS.

Table 3. Optimized dimensions of the two unit cells in mm.

Parameter	d_1	W_1	P_1	g_1	d_2	W_2	P_2	g_2
Value	14.00	3.50	14.50	0.50	18.00	4.50	18.50	0.50

Figure 9(a) shows a comparison of the simulated transmission of different layers of FSS with the simulated transmission of the proposed FSS. Figure 9(b) shows the simulated reflection phase of the proposed FSS. The simulated transmission and reflection are obtained using the Frequency Domain Solver of CST Microwave Studio with unit-cell boundary conditions and waveguide port excitation. From Fig. 9(a), it can be seen that the stop-band characteristics of the proposed FSS is a combination of the stop-band characteristics of the different layers. It can also be noticed that the first two layers are responsible for stop-band characteristics at higher frequencies, whereas the third layer is responsible for lower frequencies.

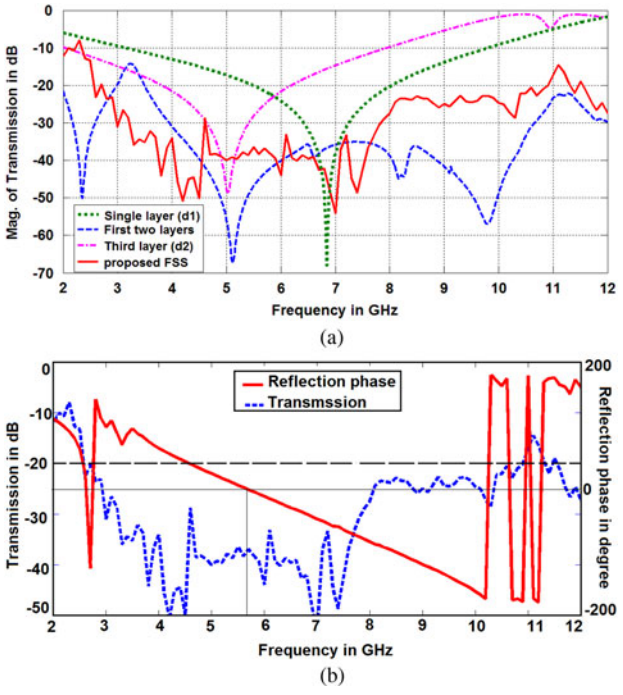

Fig. 9. (a) Comparison of the transmission response of the different layers of FSS with the proposed FSS. (b) Transmission and reflection phase response of the proposed FSS.

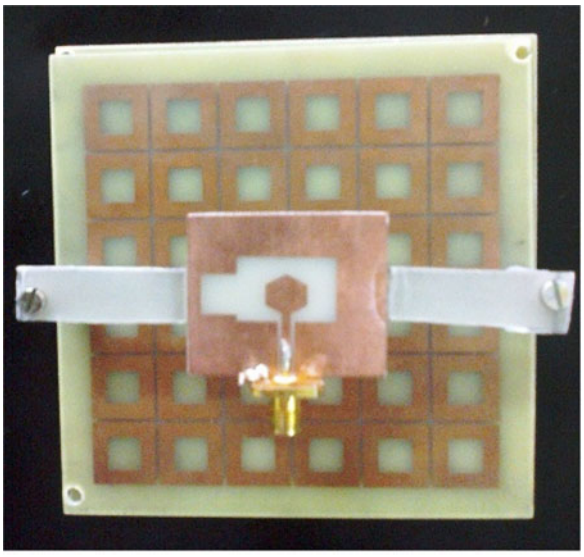

Fig. 10. Fabricated prototype of the antenna along with FSS.

V. EFFECT OF FSS ON ANTENNA CHARACTERISTICS

The proposed antenna is placed above the FSS such that the waves radiated from the antenna and waves reflected from the FSS are added and results into enhancement in the gain. The FSS is used as a reflector. The condition for the waves from antenna and reflected waves from the FSS to be in phase is given by

$$\Phi_{FSS} - 2\beta h = 2n\pi, \quad n = -1,\ 0,\ 1,\ \ldots. \tag{5}$$

Here Φ_{FSS} is the reflection phase of the FSS, β is the propagation constant in the free space and h is the distance between the patch and the FSS. From Fig. 9(b) the zero reflection phase frequency is found to be 5.7 GHz. Using equation (5), the value of h is calculated and found to be 26.31 mm. Figure 10 shows the fabricated prototype of proposed antenna along with FSS.

A) Reflection coefficient

The antenna is placed at a distance of 26.31 mm (calculated in the above subsection) above the FSS. Figure 11 shows a comparison of measured and simulated reflection coefficients of the proposed antenna without and with the FSS. It can be

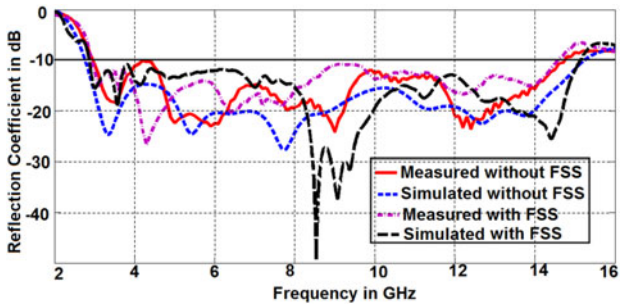

Fig. 11. Measured and simulated reflection coefficients of the antenna with and without FSS.

https://doi.org/10.1017/S1759078714000865 Published online by Cambridge University Press

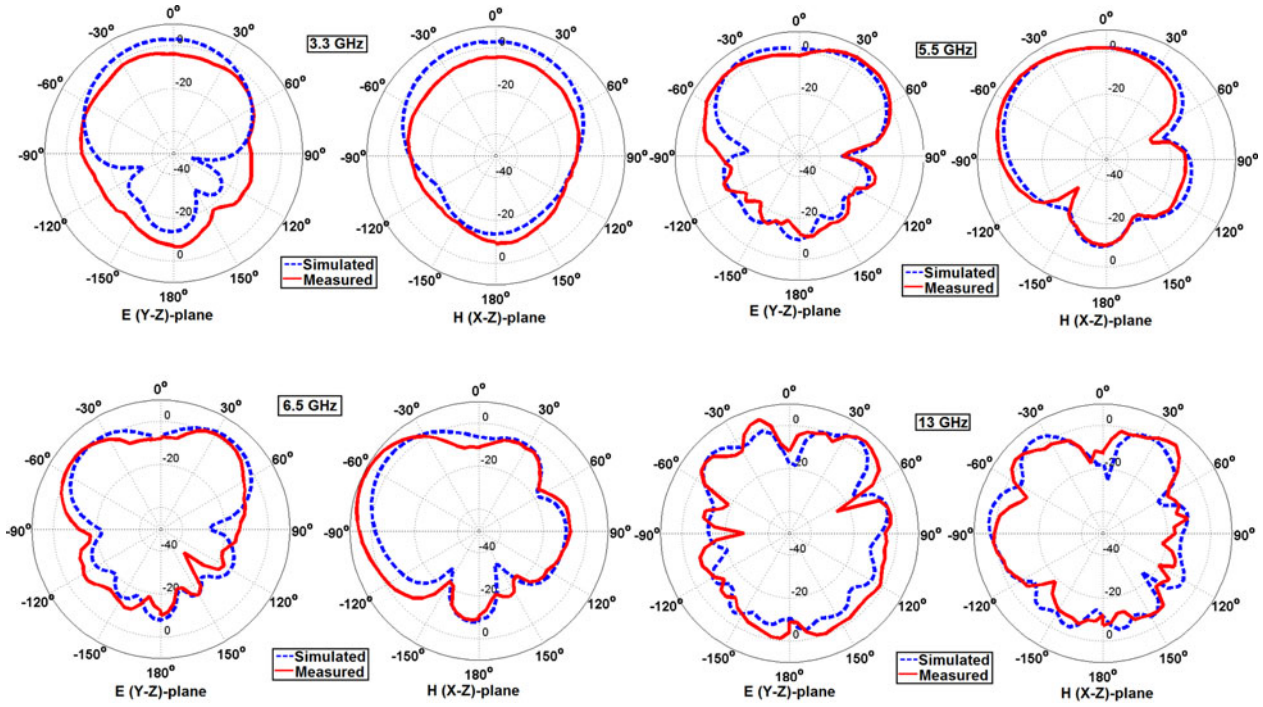

Fig. 12. Measured and simulated radiation patterns of the proposed antenna with FSS at different resonance frequencies.

seen from the figure that the measured impedance bandwidth is same in case of antenna without and with the FSS. There seems to be some misalignment (shifting in the resonance frequencies) between the simulated and measured reflection coefficients for the antenna with the FSS. This may be because the height of the FSS in the assembly may not be exactly equal to the theoretical optimum value of 26.31 mm. It can also be noticed that the return loss improves at about 4 GHz after application of the FSS. Further some extra resonances are created by the application of FSS. This may be due to the multiple reflections caused by the FSS.

B) Radiation patterns and peak gain

The proposed antenna is placed at a distance h above the FSS where h is calculated by equation (3). When the waves radiated from the antenna falls on the FSS reflector, these waves are reflected with a phase change. The phase is decided by the reflection phase of the FSS. If the distance between the antenna and the FSS is properly chosen (as calculated by equation (3)), the reradiated waves from FSS and radiated waves from the antenna are added in phase and results into higher gain and back lobe suppression. Figure 12 shows the measured and simulated radiation patterns of the antenna with the FSS. From the figure, it can be seen that the measured and simulated radiation patterns are in good agreement. By comparing with Fig. 7, it is seen that for the antenna with FSS, back lobes are also reduced. It can be also noticed from Fig. 12, that at higher frequencies the radiation patterns deviate from bi-directional nature in the *E*-plane and from omni-directional nature in the *H*-plane. Figure 13 shows the comparison of measured peak gain of the antenna without and with the FSS. It can be seen from the figure that there is 4–5 dBi gain improvement in case of antenna with FSS in comparison with the antenna without the FSS. Improvement in the gain at about 4 GHz is the maximum due to better impedance matching at this frequency.

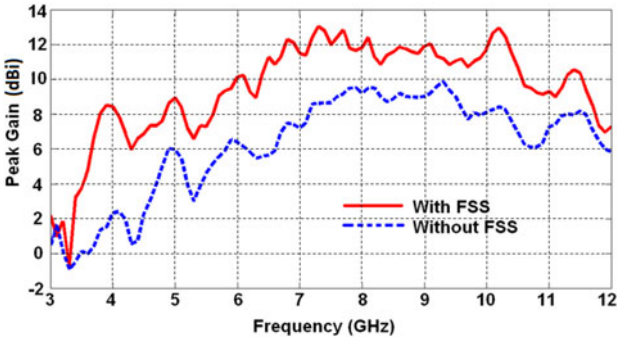

Fig. 13. Measured gain with and without FSS.

VI. CONCLUSIONS

A compact, UWB, CPW-fed slot antenna is designed. The slot is rectangular in shape with a small extension on one side. The asymmetry so created helps in wider impedance matching. The proposed antenna has a measured impedance bandwidth of 11.85 GHz from 2.9 to 14.75 GHz. The radiation patterns at different resonance frequencies are also presented. The asymmetric slot slightly affects the *H*-plane radiation patterns of the antenna particularly at mid-frequencies. To increase the gain of the proposed antenna, a three metallic layer FSS is designed and used as a reflector. There is 4–5 dBi improvement in the peak gain after application of the FSS. The measured and simulated results are in good agreement.

https://doi.org/10.1017/S1759078714000865 Published online by Cambridge University Press

ACKNOWLEDGEMENT

The authors acknowledge the Vice chancellor DIAT (DU) for the financial support.

REFERENCES

[1] Azim, R.; Islam, M.T.; Misran, N.: Compact tapered-shape slot antenna for UWB applications. IEEE Antennas Wirel. Propag. Lett., **10** (2011), 1190–1193.

[2] Liu, Y.F.; Lan, K.L.; Xue, Q.; Chan, C.H.: Experimental studies of printed wide-slot antenna for wide-band applications. IEEE Antennas Wirel. Propag. Lett., **3** (2004), 273–275.

[3] Jan, J.Y.; Su, J.W.: Bandwidth enhancement of a printed wide-slot antenna with a rotated slot. IEEE Trans. Antennas Propag., **53** (2005), 2111–2114.

[4] Thakare, Y.B.; Kumar, R.: Design of fractal patch antenna for size and radar cross-section reduction. IET Microw. Antennas Propag., **4** (2) (2010), 175–181.

[5] Liang, J.; Guo, L.; Chiau, C.C.; Chen, X.: CPW-fed circular disc monopole antenna for UWB applications, in IEEE Int. Workshop on Antenna Technology: Small Antennas and Novel Metamaterials (IWAT), 2005, 505–508.

[6] Kim, J.I.; Jee, Y.: Design of ultrawideband coplanar waveguide-fed LI-shape planar monopole antennas. IEEE Antennas Wirel. Propag. Lett., **6** (2007), 383–387.

[7] Thomas, P.; Krishna, D.D.; Gopikrishna, M.; Kalappura, U.G.; Aanandan, C.K.: Compact planar ultra-wideband bevelled monopole for portable UWB systems. Electron. Lett., **47** (20) (2011), 1112–1114.

[8] Pourahmadazar, J.; Ghobadi, C.; Nourinia, J.; Felegari, N.; Shirzad, H.: Broadband CPW-fed circularly polarized square slot antenna with inverted-L strips for UWB applications. IEEE Antennas Wirel. Propag. Lett., **10** (2011), 369–372.

[9] Qing, X.; Chen, Z.N.: Compact coplanar waveguide-fed ultra-wideband monopole-like slot antenna. IET Microw. Antennas Propag., **3** (5) (2009), 889–898.

[10] Pirhadi, A.; Bahrami, H.; Nasri, J.: Wideband high directive aperture coupled microstrip antenna design by using a FSS superstrate layer. IEEE Trans. Antennas Propag., **60** (4) (2012), 2101–2106.

[11] Ranga, Y.; Matekovits, L.; Esselle, K.P.; Weily, A.R.: Multioctave frequency selective surface reflector for ultrawideband antennas. IEEE Antennas Wirel. Propag. Lett., **10** (2011), 219–222.

[12] Ranga, Y.; Matekovits, L.; Esselle, K.P.; Weily, A.R.: Design and analysis of frequency-selective surfaces for ultrawideband applications, in IEEE Int. Conf. Computer as a Tool (EUROCON), 2011, 27–29.

[13] Gupta, K.C.; Garg, R.; Bahl, I.; Bhartia, P.: Microstrip Lines and Slotlines, Artech House, Norwood, MA, 1996.

Raghupatruni Venkat Siva Ram Krishna received the Bachelor's and Master's degrees in Electrical Engineering from Nagpur University, Nagpur, India in 1998 and 2002, respectively. Presently, he is working toward his Ph.D. degree at DIAT (Deemed University), Pune, India. Prior to joining DIAT, he worked as a faculty at the Dehradun Institute of Technology, Dehradun, India. His research area concerns wideband, dual, and circularly polarized antennas.

Raj Kumar was born on 14th May 1963 in Muzaffarnagar, UP, India. He completed his M.Sc. degree in Electronics in 1987 from the University of Meerut, Meerut, India. He was awarded the M.Tech. and Ph.D. degrees in Microwaves in 1992 and 1997, respectively from the University of Delhi South Campus, New Delhi, India. He worked at CEERI, Pilani from 1993 to 1994 as a Research Associate. From May 1997 to June 1998, he worked as an Assistant Professor at Vellore College of Engineering (VIT), Vellore. He worked in DLRL (DRDO), Hyderabad as a Scientist from June 1998 to August 2002 and later on joined DIAT, Pune and worked in the Department of Electronics Engineering till September 2012. Since October 2012, he is working in ARDE, Pune. His field of interest is microwave components, antennas, electromagnetic band-gap, frequency selective surface, filters, multiplexers, power dividers, couplers, numerical techniques, and ANN for microwave circuits and antennas.

Nagendra Kushwaha received his B.Tech. degree in Electronics and Communication from Galgotia's College of Engineering and Technology Greater Noida, UP, India in 2010. He received his M.Tech. degree in Microwave Electronics from the University of Delhi South Campus, New Delhi, India in 2012. Currently, he is with Defence Institute of Advanced Technology, Pune, India and he is working toward his Ph.D. degree. He is a student member of IEEE. His current research includes microwave and millimeter-wave circuits, especially frequency selective surface (FSS), electromagnetic band gap (EBG), metamaterials, and printed antennas.

https://doi.org/10.1017/S1759078714000865 Published online by Cambridge University Press